G.Chaudhary[1], A.Dey[2], A.K.Dey[3]

STRESS AND DELAMINATION ANALYSIS ON OVERLAPPED-GROUPED AND OVERLAPPED-DISPERSED TAPERED COMPOSITE LAMINATE

[1]Department of Mechanical Engineering, National Institute of Technology, Silchar, Assam, India, 788010.
[2]Departmentof Mechanical Engineering, National Institute of Technology Srinagar, J&K- 190006, India
[3]Department of Civil Engineering, Central Institute of Technology Kokrajhar, Assam-783370, India: ak.dey@cit.ac.in

Abstract. Modern aeronautical structure is being made of laminated composite in which plies are terminated at discrete position to provide taperness. Ply termination is called ply-drop. Thickness variation in laminates composite is achieved by changing the number of plies in proportion to the thickness change. It requires the termination of plies, within the laminate. In the present study two different ply-drop configurations have been taken for the analysis under tensile loading, these are overlapped-grouped and overlapped-dispersed. Commercial finite element software ANSYS 14.0 is used for the analysis. To construct the model geometry, layered 3-D finite element (SOLID 20 node 186) is considered which have six degrees of freedom at each node. Tsai-Wu criterion is implemented to obtain the value of failure factor for separate plies. Interlaminar stress variations along the interface of plies are determined to initialize possible delamination sites. For both configurations the value of failure factor is found to be maximum at a position of first resin pocket tip. In case of over-lapped-grouped, delamination growth occurs at a position near the thin section but in case of overlapped-dispersed it is spread over discrete positions over the laminate.

Key words: ply-drop, laminate, delamination, interlaminar stress, ANSYS, failure factor.

1. Introduction.

Composite structures are widely used in aerospace and automobile industries due to their high strength-to-weight and stiffness-to-weight ratio. These structures occupy large area with laminated composites which are fabricated from plane sheets of fibrous composite material (Fish and Vizzini 1993, Cairns et al. 1999, Varughese and Mukherjee 1997, Craig et al. 2005, Woigk et al. 2018). Thickness variations in laminates are achieved by changing the number of plies in proportion to the thickness change. It's therefore requirest termination of plies, within the laminate. Ply termination causes rise in stress leading to reduction in laminate strength, and thereby generating structural defect like delamination (Long et al. 2015, Vidyashankar, Murty2001 and Zhang et al. 2020). Numerous researchers carried out analytical investigations of laminate composites by using Finite element analysis techniques. In this study analysis was conducted by two ways in which the first method consist of estimation of stresses near the ply drops and another method consist of estimation of a fracture parameter like strain energy release rate. Currently the attention of researchers towards on taper laminate structure is increasing to improve the strength and stability (Curry et al. 1987, Carvalho et al. 2015, Wang et al. 2013, Budzik et al. 2021 and Hussain et al. 2021). One of the important factors is to design of taper itself. There are generally two different choices which are in use in designing ply-drop. First choice is the ‘grouped’ in which plies are dropped together and second is ‘dispersed’ in which one continuous ply is placed between

two dropped plies (Kim et al. 1999, Mortensen and Thomsen 2008, Woigk et al. 2021 and Gordon et al. 2021). Accordingly, Fig. 1 shows two different configurations in which plies are dropped in overlapped manner.

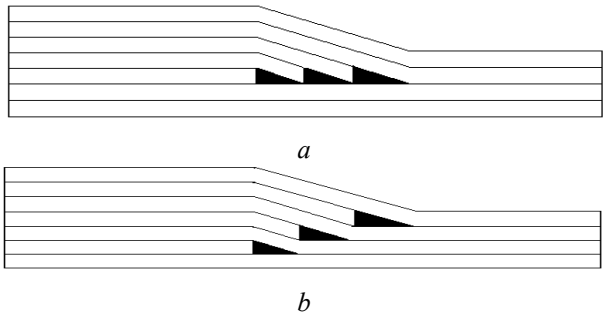

Fig. 1. Schematic drawing of ply-drop laminate,
a – overlapped-Grouped, *b* – overlapped-Dispersed.

Relatively little work appears to have been done to investigate the effect of different ply-drop configuration. Fish&Vizzini (1993) carried out experiment on glass/epoxy tapered specimens under static tension and tension-tension fatigue for four different ply-drop configurations, in which they found stair cased-grouped and dispersed-overlapped specimens exhibited preferred structural performance by retaining their bending stiffness up to failure. Cairns et al. (1999) have explored various factor for design with composite structure with ply-drop. These factors include thickness, ply stacking sequence, ply drop geometry and manufacturing considerations. In addition, fatigue loading is considered with respect to delamination initiation and growth. Varughese & Mukherjee (1997) developed a novel ply drop-off element, which consist of eight-node quadrilateral isoperametric for taper laminate composites analysis and also developed global structural matrix without increasing size. Craig and Fleck (2005) conducted an experiment on tapered laminates in presence of axial compression loading. In which they observed that mode of failures near the dropped plies are micro buckling or delamination. Vidya Shankar and Murty (2001) studied the effect of resin pockets near ply termination zone for in-plane strength, in which they identified high stress concentration zones and Effect of number of dropped plies on taper section. Kim et. al., (1999) have generated patch wise optimal layup design method for the tapered composite laminates, in which the optimal solution was obtained by integration of an expert system shell, genetic algorithm (GA) and Finite element method. Curry et al. (1987) analysed 16 ply graphite epoxy laminates with four plies dropped at the midplane using a two-stage finite element technique. An experimental study of the same laminate shows failure analysis under predicted failure load was significantly about 33%. P.D. Mangalgiri and Vijayaraju (1994) carried the finite element analysis of graphite/epoxy composite materials on a tapered beam with external dropped ply and found that delamination occurs at dropped ply near thin section. Her (2002) described a combination of analytical and numerical method to solve the ply-drop off problem by using Eigen function expansion method. Morton et al. (1994) proposed a simple method for the design and assessment of tapered laminates. Cui et al. (1994) studied of step spacing and found that small step spacing create significant effect on delamination stress, however, when the spacing is grater then certain value, the effect is negligible. They compared two extreme cases where delamination stress varies by 27%. Dhurvey and Mittal (2013) studied effect of different lay-ups and different ply drop-off ratio (Th/L) under tensile loading. Some other studies like Cairns et. al., (1999), Obata et al. (2020) and Gordon et al. (2020) has also explored the various factor for designing composite structure with ply-drop. These factors include thickness, ply stacking sequence, ply drop geometry and manufacturing considerations.

2. Materials and Method.

In present study two different ply drop configurations, overlapped-grouped (O – G), overlapped-dispersed (*O – D*) are considered as shown in Fig. 2, *a, b* respectively. For both configurations constant parameters are length of the laminate, thick and thin section, and

taper angle. Carbon fibre reinforced polymer (CFRP) as plies material and epoxy as resin pockets are taken for analysis. Table 1 and 2 shows properties of CFRP ply material and Epoxy respectively. Dropped plies and their adjacent plies are considered as selective plies for present work.

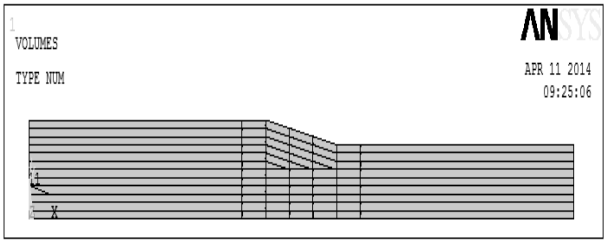

a

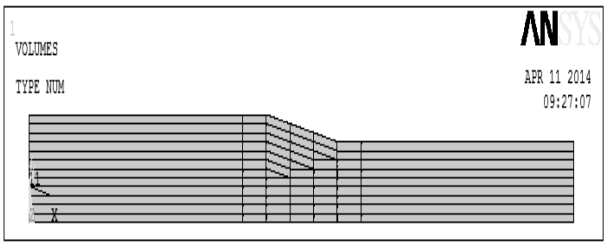

b

Fig. 2. Laminate structure, *a* – staircased-grouped, *b* – staircased-dispersed.

Table 1. Properties of CFRP ply material.

Elastic Modulus (GPa)	Shear Modulus (GPa)	Poisson's Ratio	Longitudinal Tensile and Compressive Strength (MPa)	Out of plane Tensile and Compressive Strength (MPa)	Inplane Transverse Tensile and Compressive Strength (MPa)	Shear Strength (MPa)
E_{11}=13,0	G_{12}=5,0	ν_{12}=0,35	X_T=1300	Y_T=70	Z_T=100	S_{12}=70
E_{22}=10,0	G_{23}=5,0	ν_{23}=0,35	X_C=1050	Y_C=240	Z_C=240	S_{23}=50
E_{33}=10,0	G_{13}=5,0	ν_{13}=0,35				S_{13}=95

Table 2. Properties of Epoxy.

Elastic Modulus (GPa)	Shear Modulus (GPa)	Poisson's Ratio	Tensile and Compressive Strength (MPa)	Shear Strength (MPa)
E=3,9	G=1,8	ν=0,35	X=70,0	S=50,0

Lay-up:

In case of overlapped-grouped, three plies are dropped together with lay-up configuration $[0_6 / \theta_{3D} / 0_3]$, and in case of overlapped-dispersed, plies are dropped between continuous plies with lay-up configuration $[0_5 / \theta_{1D} / 0 / \theta_{1D} / 0 / \theta_{1D} / 0_2]$. All plies have been taken at zero-degree orientation for analysis. Length of thick and thin sections are 7,5 mm each and taper section length is 2,25 mm. Taper angle is considered $11{,}3°$ for both the models. The displacement and the force boundary conditions are chosen as follows: $u = 0$ at $X = 0$, $v = 0$ at $Y = 0$ and $w = 0$ at $Z = 0$ and uniform pressure at $X = L$ on $Y - Z$ plane ($\sigma_0 = 350$ MPa). All the datum cases for numbering the plies is taken as $Y = 0$ plane.

3. Finite Element Modelling. A Finite Element Method (FEM) is used for the analysis of the configuration described in the earlier section. Commercial software package ANSYS 14.0 APDL is used in the present study. The region where plies are dropped is discredited using solid 20-noded 186 layered elements having six degrees of freedom at each node. At the ply drop area the mesh refinement is such that the smallest element is about one-third of the ply thickness ($h = 0{,}15$ mm) as shown in Fig. 3, *a, b* for overlapped-grouped and overlapped-dispersed respectively.

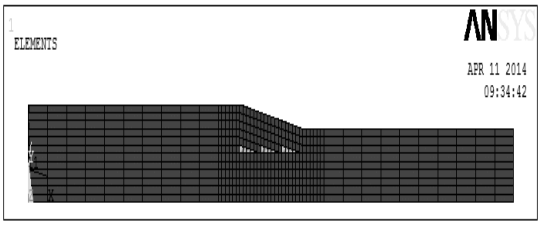

a

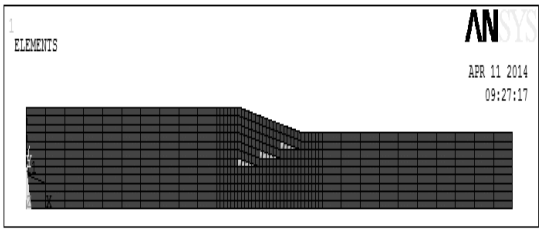

b

Fig. 3. Finite element models, *a* – staircased-grouped, *b* – staircased-dispersed.

In the present aspect, only one element is used to model in Z direction so there is no variation of stresses in the width. Failure load factor, using Tsai-Wu failure criterion given below which takes into consideration all the six components of stress and strength, are determined for different fibre orientations.

$$f = H_1\sigma_1 + H_2\sigma_2 + H_3\sigma_3 + H_{12}\sigma_1\sigma_2 + H_{23}\sigma_2\sigma_3 + H_{13}\sigma_1\sigma_3 + H_{11}{\sigma_1}^2 +$$

$$+ H_{22}{\sigma_2}^2 + H_{33}{\sigma_3}^2 + H_{44}{\sigma_4}^2 + H_{55}{\sigma_5}^2 + H_{66}{\sigma_6}^2,$$

where

$$H_1 = \frac{1}{X_T} - \frac{1}{X_C};\ H_2 = \frac{1}{Y_T} - \frac{1}{Y_C};\ H_3 = \frac{1}{Z_T} - \frac{1}{Z_C};\ H_{11} = \frac{1}{X_T X_C};\ H_{22} = \frac{1}{Y_T Y_C};\ H_{33} = \frac{1}{Z_T Z_C};$$

$$H_{44} = \frac{1}{S_{XY}^2};\ H_{55} = \frac{1}{S_{YZ}^2};\ H_{12} = \frac{1}{2}\sqrt{H_{11}H_{22}};\ H_{23} = \frac{1}{2}\sqrt{H_{22}H_{33}};\ H_{13} = \frac{1}{2}\sqrt{H_{11}H_{33}}$$

and $\{\sigma_1, \sigma_2, \sigma_3, \sigma_4, \sigma_5, \sigma_6\} = \{\sigma_{xx}, \sigma_{yy}, \sigma_{zz}, \tau_{xy}, \tau_{yz}, \tau_{xz}\}$.

At the beginning, the effect of mesh refinement on the convergence trend of stress was investigated. Hexagonal mesh is considered in this analysis. Table 3 illustrates the convergence trend for significant stress in ply no. 6 near ply drop location. The result indicates good convergence trend and small element size 0,0625 was chosen along *X* direction for all subsequent study.

Table 3. Convergence trend for significant stress.

Nodal spacing (mm)	σ_{xx} ($X = 9{,}75$ mm) (MPa)	σ_{yy} ($X = 9{,}75$mm) (MPa)	τ_{xy} ($X = 9$mm) (MPa)
0,15	417,07	29,75	– 7,86
0,0937	450,72	40,63	– 11,3
0,0625	454,55	41,7	– 12,61

4. Results and Discussion.

4.1. Stress distribution for laminate due to taper. Stress distribution contour plots for overlapped-grouped configuration are shown in Fig. 4. All the resin pockets are arranged in a line. Longitudinal stress (454,55 MPa) is higher at vicinity of resin pocket which is near the thin section compared to that of other sections of resin pockets. Maximum value of longitudinal stress is found at last belt ply. Interlaminar normal stress was observed with a maximum (41,7 MPa) at the tip of resin pocket near thin section and minimum (-27,5918 MPa) at position of first ply-drop. Value of Interlaminar shear stress under resin pocket, near thin section was observed to be maximum.

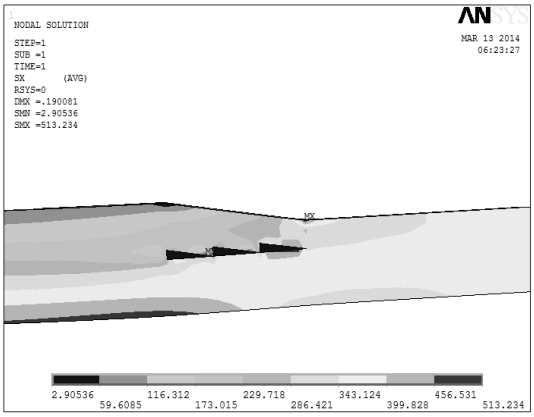

a

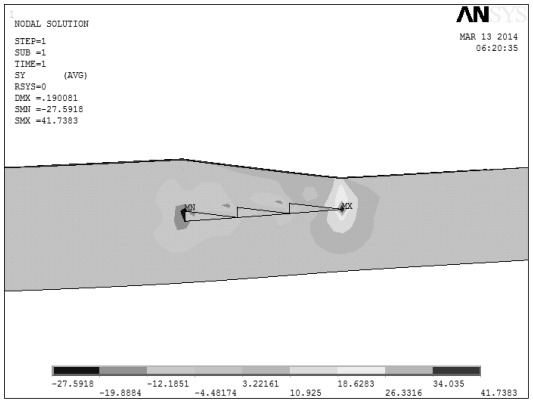

b

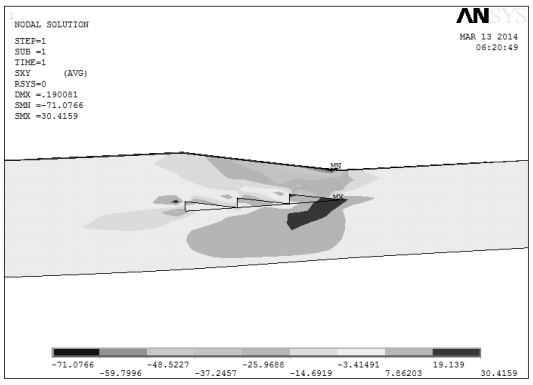

c

Fig. 4. Stress contours overlapped-grouped (O – G) ($\theta = 0°$) with taper angle $\alpha = 11{,}3$; *a* – Longitudinal stress X – direction, *b* – Normal stress Y – direction, *c* – shear stress X – Y plane.

Fig. 5 shows stress contour plots for overlapped-dispersed configuration. High value of longitudinal stress are observed near all resin pockets and observed maximum at position of first ply drop near thick sections as compared to other sections. Interlaminar stress is found positive at tip of all resin pockets. Change in sign of interlaminar shear stress is observed at the upper and lower portion of resin pockets.

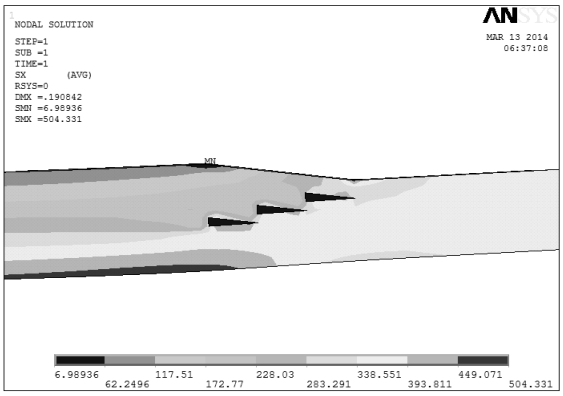

a

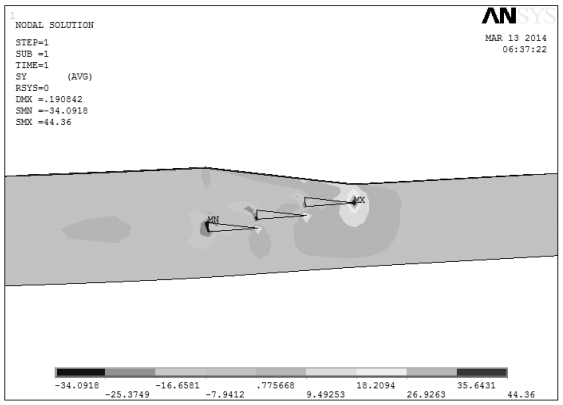

b

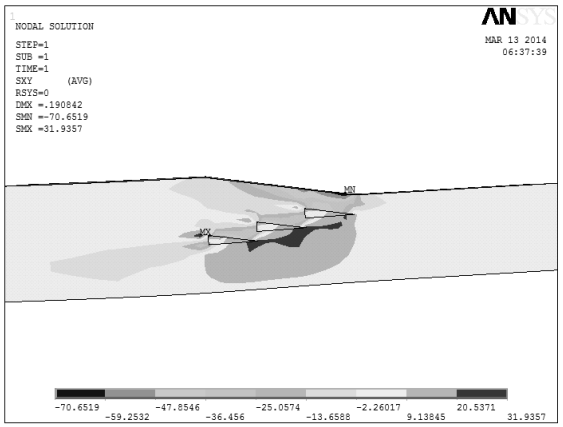

c

Fig. 5. Stress contours for overlapped-dispersed ($O - D$) ($\theta = 0°$) with taper angle $\alpha = 11{,}3$; *a* – longitudinal stress X – direction, *b* – normal stress Y – direction, *c* – shear stress $X - Y$.

4.2. Trend of Stress Distribution. Fig. 6 shows stress distribution along laminate length for selective plies which contributes to the ply-drop. Longitudinal stress, interlaminar normal and shear stress distribution for staircased-grouped and staircased-dispersed are shown in Fig. 6, *a – c* and Fig. 6, *d – f* respectively.

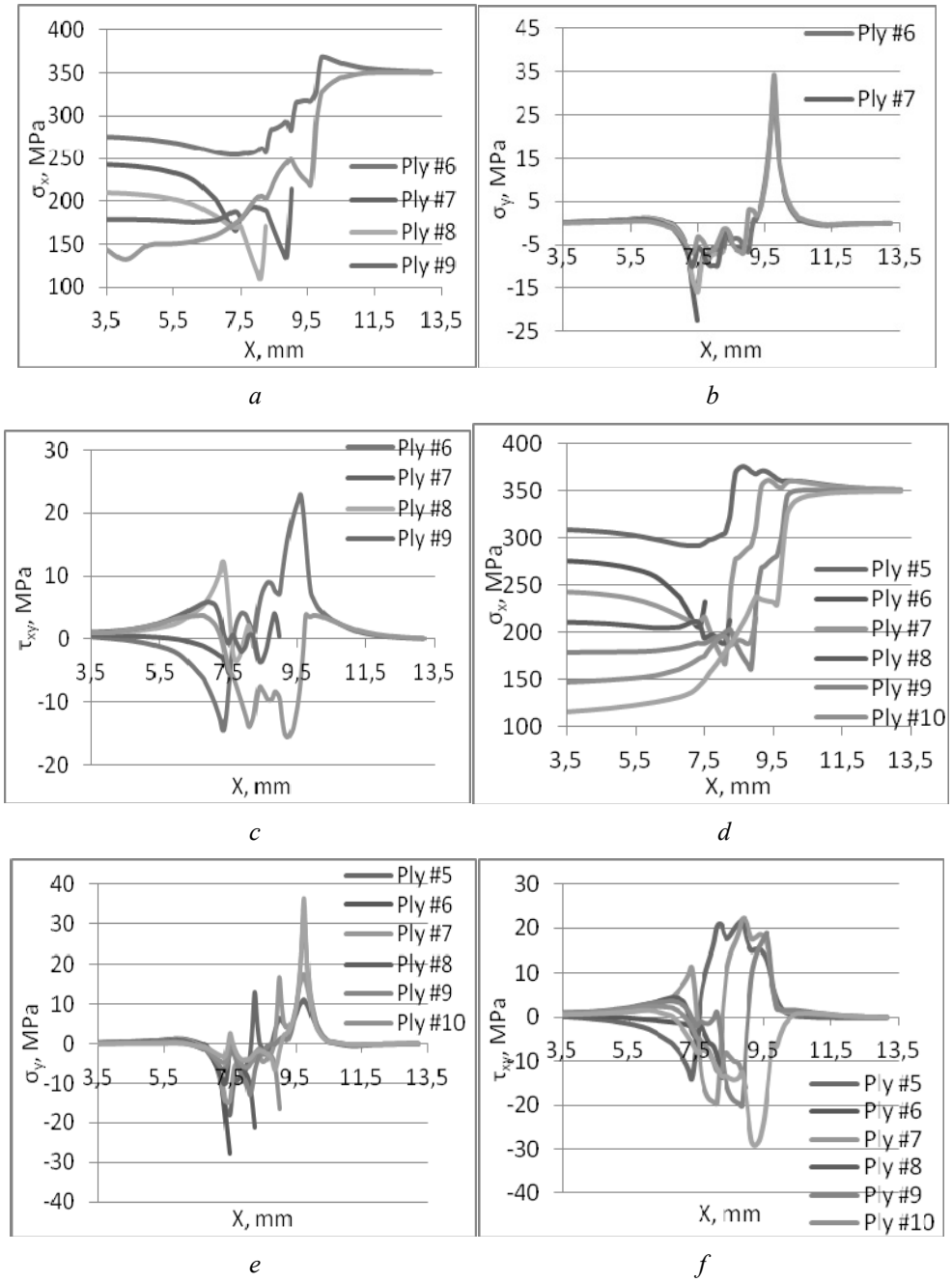

Fig. 6, a – c showing stress distribution in selective plies along length of laminate for overlapped-grouped $[0_6 / \theta_{3D} / 0_3]$.

Fig. 6, d – f showing overlapped-dispersed $[0_5 / \theta_{1D} / 0 / \theta_{1D} / 0 / \theta_{1D} / 0_2]$, $\theta = 0°$.

4.3. Failure factor Variation at the vicinity of taper using Tsai-Wu Criterion. Fig. 7 and Fig. 8 shows failure factor variation along the length for selective plies. In overlapped-grouped configuration, it is found that for plies 6 and 10 failure factor value is maximum at the tip of resin pocket near the thin section. At the starting position of taper region, value of failure factor in dropped plies is observed as significant and for first dropped ply it is the highest. In case of overlapped-dispersed, for all continuous plies at those areas where plies are dropped, significant value of failure factor is found. Maximum value of failure factor is observed in ply 11 at the tip of resin pocket.

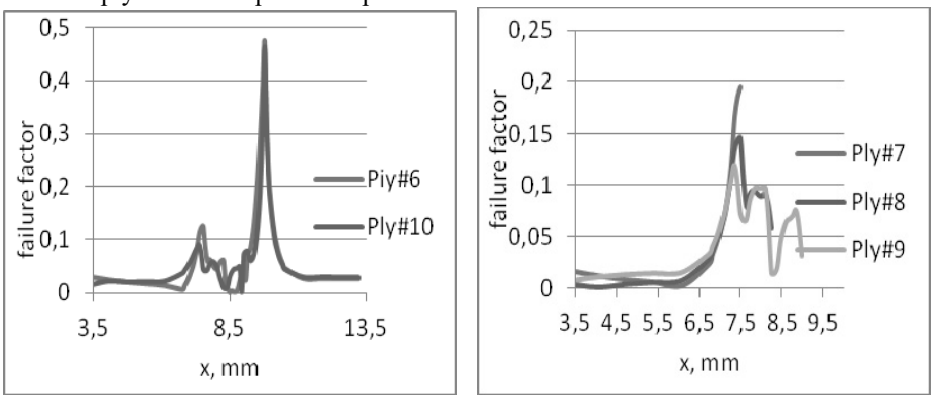

Fig. 7. Failure factor for selective plies in *O – G* configuration using Tsai-Wu criterion.

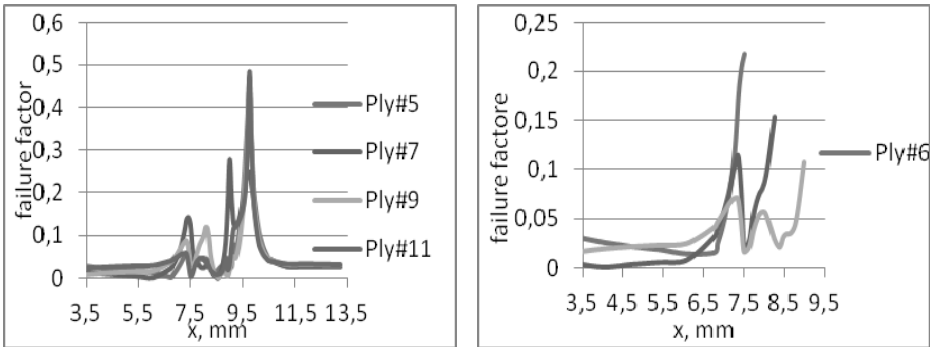

Fig. 8. Failure factor for selective plies in *O – D* configuration using Tsai-Wu criterion.

4.4. Interlaminar Stress Distribution near taper section. Interlaminar stress variations, with respect to the thickness of laminate at different positions near the taper section are determined for both configurations as shown in Fig. 9 and Fig. 10.

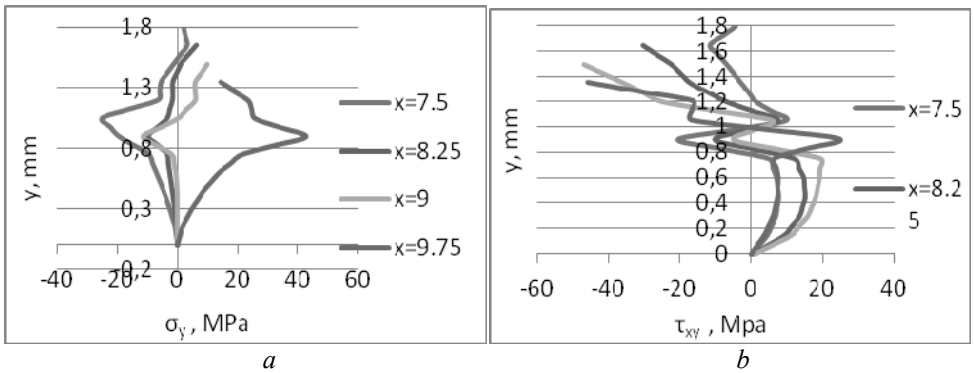

a *b*

Fig. 9. Interlaminar stress variation along thickness of laminate for *S – G* configuration, *a* – normal stress (σ_y), *b* –shear stress (τ_{xy}).

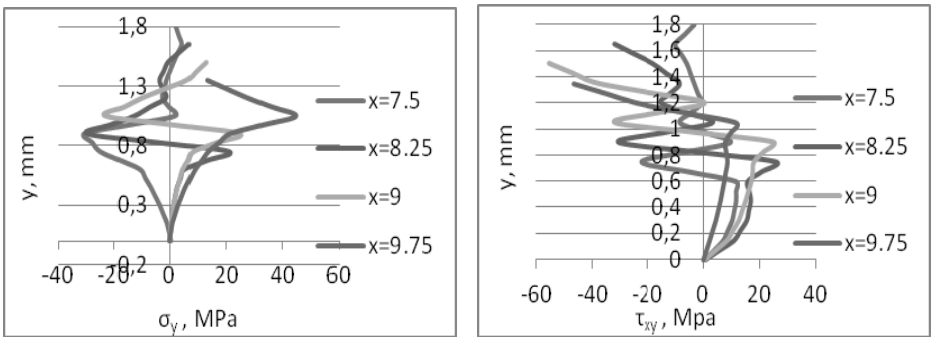

a *b*

Fig. 10. Interlaminar stress variation along thickness of laminate for *S* – *D* configuration, *a* – normal stress (σ_y), *b* – shear Stress (τ_{xy}).

For *O* – *G* configuration, high normal stress with steep gradients is found at the tip of resin pocket near thin section, which signifies maximum delamination possibility there. Again, for the same configuration, interlaminar normal stress at the tip of all resin pockets is observed as high and positive which shows possible delamination sites.

4.5. Delamination growth Prediction at the junction of selective plies. Variation of interlaminar stress at the junction of the selective plies near resin pockets are shown in Fig. 11 and Fig. 12.

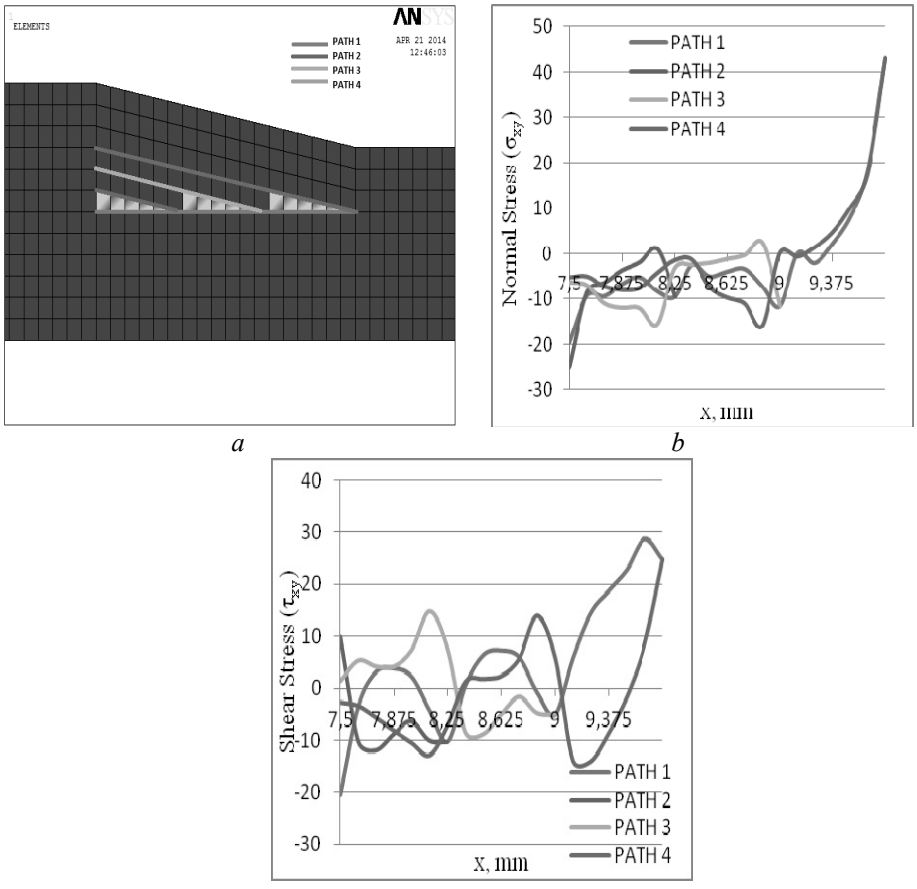

a *b*

c

Fig. 11. Interlaminar stress variation with taper length at junction of selective plies for *O* – *G* configuration, *a* – finite element model, *b* – normal Stress (σ_y), *c* – shear stress (τ_{xy}).

Interface of plies are reported with different colours. In case of overlapped-grouped, interlaminar normal stress value for PATH 2 and PATH 3 (Figures discusses about path 1 and 2) at the position which is near the tip of resin pocket is observed higher than those for the remaining paths, indicating the greatest possibility of delamination onset/growth along them. For over lapped-dispersed, for configuration at all resin pockets, Interlaminar normal stress (ILNS) values across the lower interface are found higher than those for the upper interface, indicating greatest possibility of delamination onset/growth along lower portion.

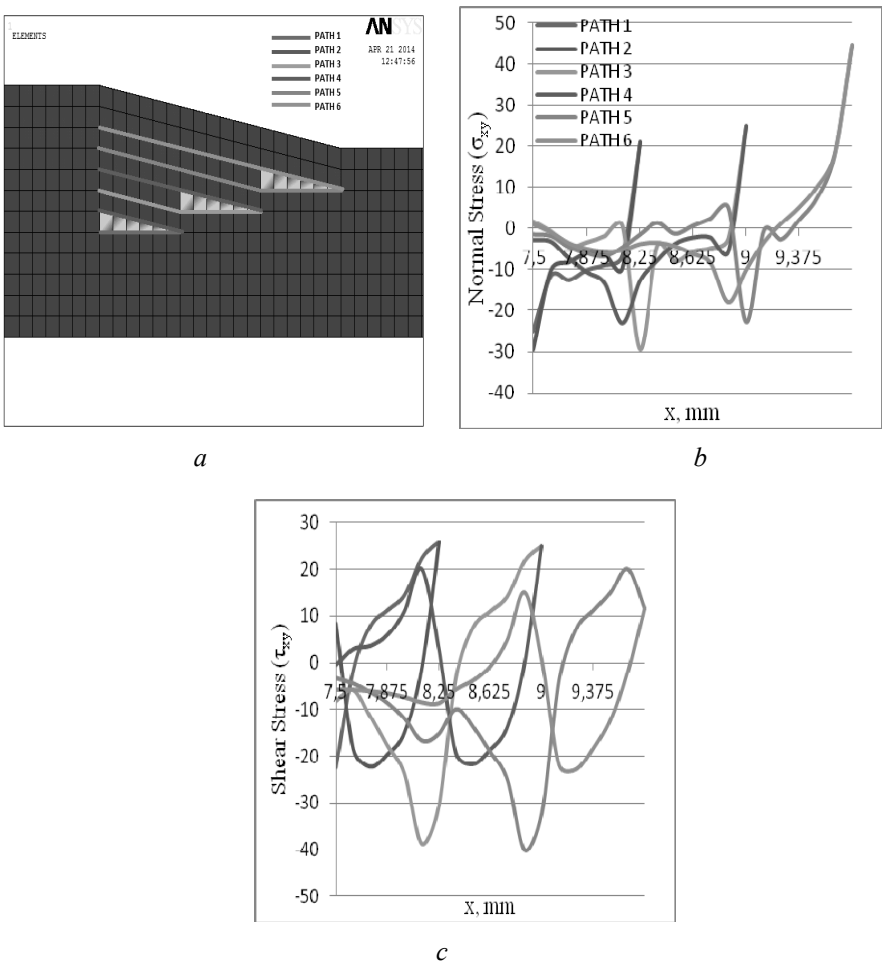

a *b*

c

Fig. 12. Interlaminar stress variation with taper length at junction of selective plies for *O* – *D* configuration, *a* – finite element model, *b* – normal stress (σ_y), *c* – shear stress (τ_{xy}).

5. Conclusions.

In the present work, stress analysis has been performed on two different ply-drop configurations of taper laminate for investigation of individual plies strength. Possible delamination sites are observed by considering interlaminar stresses. Layered 3-D finite elements are employed to model the layered zone. The variation of stresses along the length and thickness of the laminate are obtained. Tsai-Wu failure criterion has been used for determination of failure factor for individual plies. Inferencesof results indicates the following

Stress concentration was found at the vicinity of resin pockets.

Longitudinal stress value for both the models were observed high at the position of resin pocket, near thin section.

For both the models, longitudinal stress value is found to be maximum at the last belt which shows that there may be local bending present at outer belt ply.

Steep gradients of interlaminar stresses are noted in the taper region, suggesting the vulnerability of these sites for delamination onset/growth.

Value of failure factor was observed high at ply-drop position, indicating load transfer mechanism of dropped plies to adjacent plies.

In case of overlapped-grouped (*O – G*), interlaminar normal stress was found maximum and positive at the tip of resin pocket near thin section indicating possible delamination site.

In case of overlapped-dispersed (*O – D*), interlaminar normal stress was found significant and positive for all resin pocket tips, suggesting delamination sites are spread at discrete positions inside the laminate.

For overlapped-dispersed, all the configuration ILNS values across the lower interface were found higher than those for the upper interface for all resin pockets, indicating greatest possibility of delamination onset/growth along lower portion.

РЕЗЮМЕ. Сучасна аеронавігаційна конструкція виготовляється з ламінованого композиту, шари якого закінчуються в окремих положеннях для забезпечення конусності. Завершення шару називається падінням шару. Зміна товщини ламінатного композиту досягається зміною кількості шарів пропорційно зміні товщини. Це вимагає закінчення шарів всередині ламінату. У цьому дослідженні для аналізу при навантаженні на розтяг було взято дві різні конфігурації падіння шару: перекрито-згруповані і перекрито-розсіяні. Для аналізу використовується комерційне програмне забезпечення скінчених елементів ANSYS 14.0. Для побудови геометрії моделі розглядається багатошаровий тривимірний скінчений елемент (вузол 186 SOLID 20), який має шість ступенів свободи в кожному вузлі. Критерій Tsai-Wu реалізований для отримання значення коефіцієнта руйнування для окремих шарів. Міжшарові варіації напружень вздовж поверхні поділу шарів визначаються для ініціалізації можливих місць розшарування. Для обох конфігурацій встановлено, що значення коефіцієнта руйнування є максимальним у положенні першого накінечника полімерної кишені. У випадку згрупування перекриття розшарування відбувається в місці поблизу тонкої ділянки, але у випадку з розсіяння перекриттям воно поширюється на окремі позиції по ламінату.

КЛЮЧОВІ СЛОВА: падіння шару, ламінат, розшарування, міжшарове напруження, ANSYS, коефіцієнт руйнування.

1. *Fish J.C., Vizzini A.J.* Delamination of ply-drop configurations // Composite Material Testing and Design. – 1993. – **11**. – P. 323 – 332.
2. *Woigk W., Hallett S.R., Jones M.I., Kuhtz M., Hornig A., Gude M.* Experimental investigation of the effect of defects in Automated Fibre Placement produced composite laminates // Composite Struct. –2018. – **201**. – P. 1004 – 1017.
3. *Cairns D.S., Mandell J.F, Scott M.E.* Design and manufacturing consideration for ply drops in composite structures // Composites. Part B. – 1999. – **30**. – P. 523 – 534.
4. *Varughese B., Mukherjee A*. A ply drop-off element for analysis of tapered laminated composites // Composite Struct. – 1997. – **39**, N 1 – 2. – P. 123 – 144.
5. *Steeves C.A., Fleck N.A.* Compressive strength of composite laminates with terminated internal plies // Composites. Part A. – 2005. – **36**. – P. 798 – 805.
6. *Long S., Yao X., Zhang X.* Delamination prediction in composite laminates under low-velocity impact // Composite Struct. – 2015. – **132**, N 15. – P. 290 – 298.
7. *Vidyashankar B.R., Krishna Murty A.V.* Analysis of laminate with ply drops // Composite Sci. and Technology. – 2001. – **61**. – P. 749 – 758.
8. *Zhang B., Kawashita L.F., Jones M.I., Lander J.K., Hallett S.R.* An experimental and numerical investigation into damage mechanisms in tapered laminates under tensile loading // Composites. Part A: Appl. Sci. and Manufacturing. – 2020. – **133**. – 105862.
9. *Curry J.M, Johnson E.R., Starnes Jr.J.H.* Effect of dropped plies on the strength of graphite-epoxy laminates // Proc. of AIAA/ ASME/ASCE/AHS/ASC 29th Structures, Structural Dynamics, Materials Conf. Part I, Monterey, CA. – 1987. – AIAA paper N 87-084. – P. 737 – 47.
10. *De Carvalho N.V., Chen B.Y., Pinho S.T., Ratcliffe J.G., Baiz P.M., Tay T.E.* Modeling delamination migration in cross-ply tape laminates // Composites. Part A: Appl. Sci. and Manufacturing. – 2015. – **71**. – P. 192 – 203.

11. *Wang J., Potter K.D., Etches J.* Experimental investigation and characterisation techniques of compressive fatigue failure of composites with fibre waviness at ply drops // Composite Struct. – 2013. – **100**. – P. 398 – 403.
12. *Kim J.S., Kim C.G., Hong C.S.* Optimum design of composite structures with ply drop using genetic algorithm and expert system shell // Composite Struct. – 1999. – **46.** – P. 171 – 187.
13. *Mortensen F., Thomsen O.T.* Simple and efficient interlaminar stressanalysis of composite laminates with internal ply-drop // Composite Struct. – 2008. – **84**, N 1. – P. 73 – 86.
14. *Mangalgiri P.D., Vijayaraju K*. An analytical study on 0/90 ply-drops in composite laminate. – Composite Struct. – 1994. – **28**. – P. 181 – 185.
15. *Her S.C*. Stress analysis of ply drop-off in composite structure // Composite Struct. – 2002. – **57**. – P. 235 – 244.
16. *Pernice M.F., De Carvalho N.V., Ratcliffe J.G., Hallett S.R.* Experimental study on delamination migration in composite laminates // Composites. Part A: Appl. Sci. and Manufacturing. – 2015 – **73**. – P. 20 – 34.
17. *Budzik M.K, Jorgensen S.H., Aghababaei R.* Fracture mechanics analysis of delamination along width-varying interfaces // Composites. Part B: Engineering. – 2021. – **215**. – 108793.
18. *Hussain M., Abdel-Nasser Y., Banawan A., Ahmed Y.M.* Failure analysis of tapered composite propeller blade // Ocean Engng. – 2021. – **236**. – 109506.
19. *Morton S.K., Webber J.P.H., Thomas D.M.* Design and Assessment of Composite Tapered Laminated Plates // Department of Aerospace Engineering. Department of Engng. Mathem. – 1994. – P. 2763 – 2773.
20. Cui W., Wisnom M.R., Jones M.I. Effect of step spacing on delamination of taper laminates // Composite Sci.and Technology. – 1994. – **52**. – 39 – 46.
21. *Dhurvey P.*, *Mittal N.D.* Study the effect of externally and internally ply drop-off in composite laminate analysis // ARPN J. Eng. and Appl. Sci. – 2013. – **8**, N 4.
22. *Cairns D.S., Mandell J.F., Scott M.E.* Design and manufacturing consideration for ply drops in composite structures // Composites. Part B. – 1999. – **30**. – P. 523 – 534.
23. *Yang J., Song B., Zhong X., Jin P.* Optimal design of blended composite laminate structuresusing ply drop sequence // Composite Struct. – 2016. – **135**. – P. 30 – 37.
24. *Irisarri F.X., Lasseigne A., Leroy F.H, Riche R.Le.* Optimal design of laminated composite structures with ply drops using stacking sequence tables // Composite Struct. – 2014. – **107**. – P. 559 – 569.
26. *Liu P.F., Hou S.J., Chu J.K., Hu X.Y., Zhou C.L., Liu Y.L, Zheng J.Y., Zhao A., Yan L.* Finite element analysis of postbuckling and delamination of composite laminates using virtual crack closure technique // Composite Struct. – 2011. – **93**, N 6. – P. 1549 – 1560.
26. *Woigk W., Zhang B., Jones M.I., Kuhtz M., Hornig A., Gude M., Hallett S.R.* Effect of saw-tooth ply drops on the mechanical performance of tapered composite laminates // Composite Struct. – 2021. – **272**. – 114197.
27. *Gordon T., Xu X., Kawashita L., Wisnom M.R., Hallett S.R, Kim B.C.* Delamination suppression in tapered unidirectional laminates with multiple ply drops using a tape scarfing technique // Composites. Part A: Appl. Sci. and Manufacturing. – 2021. – **150**. – 106627.
28. *Obata S., Takahashi K., Inaba K.* Laminate design for a tapered FRP structure with ply drop-off based on yielding of resin pockets // Composite Struct. – 2020. – **253**. – 112787.
29. *Gordon T., Xu X., Wisnom M.R., Kim B.C.* Novel tape termination method for automated fibre placement: Cutting characteristics and delamination suppression // Composites. Part A: Appl. Sci. and Manufacturing**.** – 2020. – **137**. – 106023.

From the Editorial Board: The article corresponds completely to submitted manuscript.

Надійшла 16.06.2021 Затверджена до друку 19.07.2022
